

Ouachita Baptist University

Scholarly Commons @ Ouachita

Honors Theses

Carl Goodson Honors Program

2019

Passive Solar Tracking Using Shape Memory Alloys

Keeley G. Johnson

Ouachita Baptist University

Follow this and additional works at: https://scholarlycommons.obu.edu/honors_theses



Part of the [Physics Commons](#)

Recommended Citation

Johnson, Keeley G., "Passive Solar Tracking Using Shape Memory Alloys" (2019). *Honors Theses*. 721.
https://scholarlycommons.obu.edu/honors_theses/721

This Thesis is brought to you for free and open access by the Carl Goodson Honors Program at Scholarly Commons @ Ouachita. It has been accepted for inclusion in Honors Theses by an authorized administrator of Scholarly Commons @ Ouachita. For more information, please contact mortensona@obu.edu.

SENIOR THESIS APPROVAL

This Honors thesis entitled

“Passive Solar Tracking Using Shape Memory Alloys”

written by

Keeley G. Johnson

and submitted in partial fulfillment of
the requirements for completion of
the Carl Goodson Honors Program
meets the criteria for acceptance
and has been approved by the undersigned readers:

Dr. Angela Douglas, thesis director

Dr. Kevin Cornelius, second reader

Dr. Barbara Pemberton, third reader

Dr. Barbara Pemberton, Honors Program director

April 23, 2019

Ouachita Baptist University

Passive Solar Tracking Using Shape Memory Alloys

Keeley G. Johnson

Honors Thesis

2019

Acknowledgements:

I would like to thank the Dr. J.D. Patterson Summer Research Program for the opportunity to participate in undergraduate research. I would also like to thank the Physics department at Ouachita Baptist University for allowing me to do research in their department and use their materials. Specifically, I would like to thank my research advisor, Dr. Angela Douglass, for her guidance, assistance, and patience. Finally, I would like to thank the Carl Goodson Honors Program for the opportunity to investigate solar panels, shape memory alloys, and tracking mechanisms through this thesis.

Table of Contents:

Introduction: 5

A Brief History of Solar Power: 6

How Solar Panels Produce Electricity: 7

Types of Solar Panels: 8

A Discussion of Solar Tracking: 9

Two Types of Solar Tracking- Active and Passive: 12

Shape Memory Alloys: 13

Project: 15

Choosing and Testing a Shape Memory Alloy: 15

The Motor: 16

System Specifications: 19

System Calculations: 20

Efficiency Analysis: 21

Results: 24

Appendix 1: Efficiency Data Instruction Manual: 26

Appendix 2: A Discussion of Gear Trains and Inquiry into their Applications for Solar Tracking Motors: 37

Appendix 3: Efficiency Data: 41

Image Credits: 45

Bibliography: 46

Introduction:

The world's energy demands are growing daily in conjunction with the global population and urbanization. In the modern era, the main source of energy has come from nonrenewable fossil fuels. While this source is one of the cheapest forms of energy, it is also one of the worst for the environment, and will only last until the earth runs out of these fossil fuels. Solar energy, on the other hand, is both much better for the environment and an inexhaustible resource. The primary issue that arises with the accessibility of solar energy is that it is much more expensive per watt of power when compared to other sources like oil. However, solar power could become more affordable by increasing the efficiency with which it is generated, and one of the most promising methods of doing so is by solar tracking¹.

In this study, a novel passive tracker was designed and tested with the purpose of increasing solar panel efficiency. Intending to build a low maintenance, low cost, stand-alone system for powering a street light, the design was fabricated and tested against a fixed solar panel system for comparison.

Of specific interest in the project was the motor used to drive the solar tracker. The tracking mechanism designed in this research differed from other trackers because it was passive, inexpensive, utilized shape memory alloys, and increased overall power output and efficiency without requiring any extra power input. Other passive trackers have been designed using shape memory materials, photodiodes, bimetallic strips, and volatile gases. This design employed shape memory alloy springs and Fresnel lenses to drive the motor.

Efficiency was tested versus fixed panels by mimicking the angle a tracker would have set the panel to, and measuring the power output at both this angle and at a fixed solar panel's orientation. Analyses of the results showed an increased power output such that the percent difference relative to fixed solar panel systems was, on average, 62.77%. While this high percentage is indicative of the energy

gain potential on sunny days, not overcast or rainy days, it does confirm quantitatively that solar tracking is beneficial in the geographical region of interest in the project, Arkadelphia, Arkansas.

In addition to detailing the design process and efficiency testing of the solar panel tracking mechanism, background investigation into shape memory alloys and solar panels will be discussed, and a brief inquiry into gear train mechanisms that were analyzed as being potentially beneficial to the motor design will be summarized.

A Brief History of Solar Power:

The concept of harnessing solar energy originally came into practical use at the introduction of the first photovoltaic module in 1954 by Bell Laboratories. Advertised as a “solar battery,” what was first more of an interesting novelty than an innovation was adopted by the space program and developed through the next decade. As cost declined and reliability improved, the 1970s energy crisis drove a need for sustainable energy sources, pushing solar power toward becoming a legitimate, mainstream energy source. Solar panels have been the subjects of consistent innovation and improvement with regard to their technology, application, and efficiency. Now much more sophisticated than that first “solar

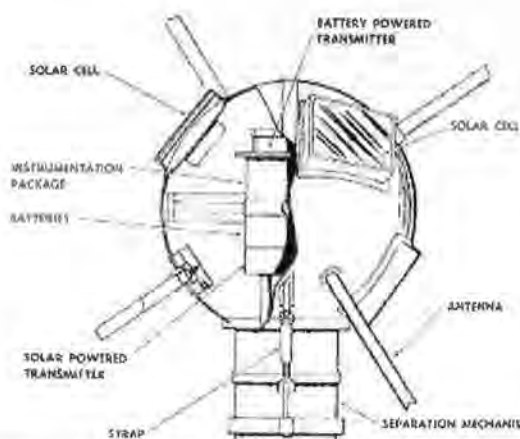


Figure 1: Technical drawing of Vanguard 1, NASA's first space craft to utilize solar power.

battery” or the small panels used on the Vanguard 1 (Figure 1), NASA’s first solar powered space craft, solar panels have an incredible variety of uses, from calculators to the gorgeous solar arrays powering modern space craft²⁻⁴. The first solar panel tracking mechanism was introduced by C. Finster in 1962, and since then

automation and technical precision have given rise to significant energy-gain potential with the use of sun tracking on solar panel systems⁵.

How Solar Panels Produce Electricity:

The underlying idea behind solar panels is the conversion of solar energy into power via electron stimulation. Through a physical phenomenon commonly known as the “photoelectric effect,” certain types of matter can absorb the energy of the photons of incident light into their electrons, and with sufficient energy the electrons will break loose from their atoms, becoming free electrons. This process is called emission. When electrons move from where they are emitted toward another material or area, a current is produced. In order for the electrons to be drawn away, however, there must be some kind of charge imbalance that induces them. Technically, a constant charge imbalance is known as an electric field, and with any electric field comes voltage. With both current production and voltage, a system will produce power^{2,6,7}.

Such a system has been designed in solar panel cells using silicon. Silicon functions as a semiconductor, and in its crystal form has a tightly compact structure. During the manufacturing process, an electric field is artificially created in the silicon wafers. Using a process called “doping,” silicon is seeded with impurities. Boron is added to molten silicon to create an electron deficiency, and crystalized silicon wafers are treated with phosphorous gas to create an excess of electrons on the outside surface of the wafer. That excess is dispelled on the back surface by depositing an aluminized conducting material onto it, leaving an excess of electrons on the top surface and deficiency of electrons in the core of the cell. The silicon regions with spare electrons are called N-type (“negative”), and the regions with holes that can be filled by electrons are called P-type (“positive”)^{2,7,8}.

Light incident on a solar panel cell makes contact with the front, N-type surface of the cell which has many extra electrons. Each photon with adequate energy frees an electron from a silicon atom, but the extra electrons will be freed more easily than a bound electron. The freed electrons move toward the P-type silicon. Between the two types of silicon, however, a boundary called a "junction" is in place. At this boundary an equilibrium exists between the positive and negative sides, but if an electron crosses over the junction it disrupts the electrical neutrality, and the electric current flows into the conductors attached to the cell, producing electricity. The current produced depends on how much sunlight is incident on the cell. The current is then directed to a battery where it is stored and can be used for power as needed^{2,6,7}.

Types of Solar Panels:

There are 2 main types of solar panel cells: monocrystalline and polycrystalline. They are easily distinguishable by their appearance, since monocrystalline cells are a much darker black color than the blue of polycrystalline, and also have distinctive rounded corners. On average, monocrystalline panels are about 2% more efficient than polycrystalline, but surprisingly one of the primary differences between them is production method, not function. The silicon cells, or segments, that make up all solar panels are cut from larger, silicon ingots. It is in the processes by which the ingots are made that the compositional difference is found. Both processes begin with either quartzite gravel or crushed quartz (used for their silicon dioxide) being melted in a furnace to recover the products carbon dioxide and silicon. The molten silicon that is recovered is subjected to purification before use in either production technique. At this stage trace amounts of boron are added to the purified, melted silicon¹¹⁻¹³.

Monocrystalline ingots are made by seeding the melted silicon slush with a seed crystal. The crystal is lowered into the slush slowly, and then rotated while it is being pulled back out. Leaving

impurities behind, much as in a smaller scale recrystallization procedure, a single crystalline structure forms around the seed crystal. The result of this process, known as the Czochralski method, is a high grade silicon ingot. To produce the individual cells the sides of the cylinder are cut off, giving the monocrystalline cells their characteristic shape, and the cylinder is then sliced into thinner “wafers,” which are about as thick as a piece of paper. Monocrystalline cells are highly efficient, but consequently are more expensive than polycrystalline cells¹¹⁻¹³.

Conversely, polycrystalline ingots are made by a simpler technique that does not require the Czochralski method. Purified silicon rocks are melted together, and poured into square shaped molds. After cooling, these ingots can be cut into wafers. The cooling process of these silicon ingots leads to the formation of many different crystals in the ingot. These crystals that make up the ingot give the resulting wafers a mottled, variegated look. Further, the disrupted surface of the wafers compared to monocrystalline wafers reduces the amount of solar energy which can be absorbed and converted into energy by the cell, reducing the overall efficiency of the panel. Thus, polycrystalline panels are generally cheaper but less efficient than monocrystalline panels^{8,11,12}.

The two techniques converge again after wafers are cut from the ingots. The wafers, nearly molten, are treated with phosphorous gas, which works its way into the silicon through the expanded gaps in the crystalline structure that are caused by the near liquid state of the wafers. After affixing conductors to each side, the cells are wired together into modules, and multiple modules can be wired together to create an array¹³.

A Discussion of Solar Tracking:

The purpose of a solar panel tracker is to rotate a solar panel such that it is directly in line with the sun at any given time. Doing so increases the output current, and consequently the output energy,

of the solar panel system significantly as compared to a fixed panel (one which has no tracking capability). While not uncommon, tracking mechanisms are also not mainstream. This is because the cost of solar energy per watt, already greater than consumable energy sources like fuel, increases with added construction cost. Having solar panels that rotate with the sun can also pose a problem for solar farms: to keep the panels from casting shadows on one another, which would significantly decrease the current output of the shaded panel, the panels must be installed farther apart than fixed panels. This increases the energy cost as more land is required to house the same number of panels. Although trackers add efficiency to the energy production, on a large scale they can cause problems like these that need to be addressed. Building tracking mechanisms for solar farms, then, is a cost with little benefit at this time. With further development, however, the issues surrounding trackers can be addressed, the efficiency of solar systems improved, the cost of solar energy decrease, and the accessibility to renewable energy increase. The designing of new tracking mechanisms that are low cost, small, or highly efficient, is a starting point for research in this area.

Trackers turn solar panels toward the sun, but to do that they have to locate the sun. Alignment of the panel is calculated with geometry. As shown in Figure 2, first the ray from the sun that is incident on the panel is projected to a horizontal surface (the ground), and the angle between the projection and geographic south is measured. This is the *solar azimuth angle*, ψ . The same is then done with a

horizontal surface projection of the normal line from the plane of the solar panel, and the angle between it and geographic south. This represents the *panel azimuth angle* (not pictured). The goal of tracking is

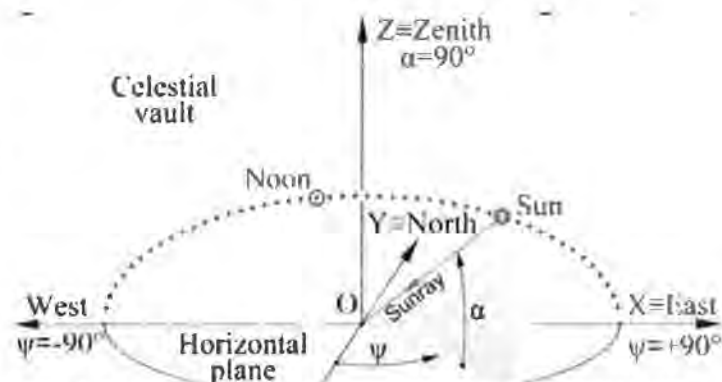


Figure 2: ψ represents the solar azimuth angle and α represents the solar elevation angle.

to align the panel such that these two angles are equal, as this will ensure the panel is directly in line with the sun in the east-west plane.

These calculations can then be used to design a tracking mechanism programmed to turn the panel accordingly. This method is particularly useful on days where the sun cannot be clearly seen due to rain, cloud cover, fog, or other inclement weather. Conversely, the calculations can be used to construct a tracker whose movement is influenced by the sun. This movement can be manipulated such that it always aligns the panel with the solar azimuth angle.

Using a similar process, a tracker could be designed to maintain its line with the sun in the north-south plane as well. This addition would make the tracker a "dual-axis" tracker, rather than "single-axis." Dual-axis trackers do provide a slight gain in efficiency compared to single-axis, but this efficiency gain varies dependent on the latitudinal location of the solar system. A measure of whether a dual-axis tracker will be beneficial over a single-axis in a given region can be found from the average clearness index of the region. The clearness index is a quantitative percentage of how much sun is irradiated on the earth, and how much is scattered due to cloud cover. The scale ranges from 0 to 1. Regions with a high clearness index are more often sunny than regions with a low clearness index.

Previous research⁵ has shown that trackers do not have to be exact with their angles, as an error of 10° can still generate an output of 98.5% of the energy possible. Even with error, tracking still increases current output as compared to non-tracking solar systems. The amount by which efficiency increases is strongly dependent on the specific tracking configuration, location in the world, and season. Each proposed mechanism of solar tracking has its own set of priorities in design, as well as performance strengths and downfalls. As the field is still emerging, research has not yet encompassed a broad enough scope to determine which method is the "best." That is to say, it is unclear which method typically has

the best ratio of performance to cost to complexity and so on, because the possibilities for how a tracker could be constructed are still being explored.

Two Types of Solar Tracking- Active and Passive:

There are two basic categories of tracking: "active" and "passive." Active tracking involves a mechanism which depends on an external energy source to power the solar panel as it turns to follow the sun. This could be a battery-powered motor on a timer, or some other such device. If power to move the tracker is harnessed from a source other than the sun, it is considered active tracking.

Passive tracking, on the other hand, utilizes a mechanism that does not require any kind of external power input to drive tracking. Power could theoretically be diverted from the solar panel itself or gained from the sun. It could also be input from thermal conductivity, or any other naturally derived differential that could drive the mechanical work of turning the panel.

While passive tracking mechanisms are often cheaper, since they do not require a consistent input of power to drive their motion, active tracking mechanisms can be more accurate. For example, a passive tracker that is dependent on direct sunlight to drive its rotation may have considerable trouble following the angle of the sun on a cloudy day. An active tracker, however, which often may be set on a timer, will follow the same path it would any other day. This will increase its overall output relative to the passive tracker because it is keeping a consistent angle with the sun throughout the day, while a passive tracker of this kind could not without direct sunlight.

Even though passive trackers might not always have as great a power output as active trackers, they are still highly efficient and provide a theoretical increase of up to 40% in power as compared to a fixed solar panel system.

Further, an active tracker will generally require more maintenance than a passive one because it is more likely to be constructed from parts which are subject to corrosion from the elements, such as electronics and metals. The mechanics may be delicate enough that they are disrupted over time from debris and storms. The tracker may run on a battery that has to be recharged periodically. Generally, then, these trackers are more complex in design, and are therefore more dependent on upkeep. Thus, an active tracker may not be able to withstand functioning in the elements for long before needing part repair or replacement.

With consideration as to the goal this research presented overall, designing a solar panel system to power a rural streetlight, focus was set on designing a passive tracker. Compared to an active one, this tracker would be lower in expense, comparably efficient, simple, and most convincingly, require little maintenance. Since the solar panel design was intended for eventual use on top of a street light, access to the mechanics would be limited and inconvenient. The system would thus be entirely self-contained, and could be placed in a location a traditional street light would be difficult to install in.

Shape Memory Alloys:

Shape memory alloys were investigated for potential use in the tracking system being designed. A shape memory alloy is a metal fabricated from more than one elemental metal (often mixture of nickel and titanium) that is capable of returning to a "preset" or "remembered" shape when heat is applied after the metal has been deformed. For example, a shape memory alloy that is made to be a straight wire is bent in half. While applying heat to any other metal would only make the wire very hot, applying heat to this shape memory alloy wire will cause it to straighten out back into its original shape. This phenomenon is the result of a property unique to shape memory alloys: 2 separate solid states.

Metals typically have gas, liquid, and solid states of being, but shape memory alloys (SMAs) have an additional solid state.

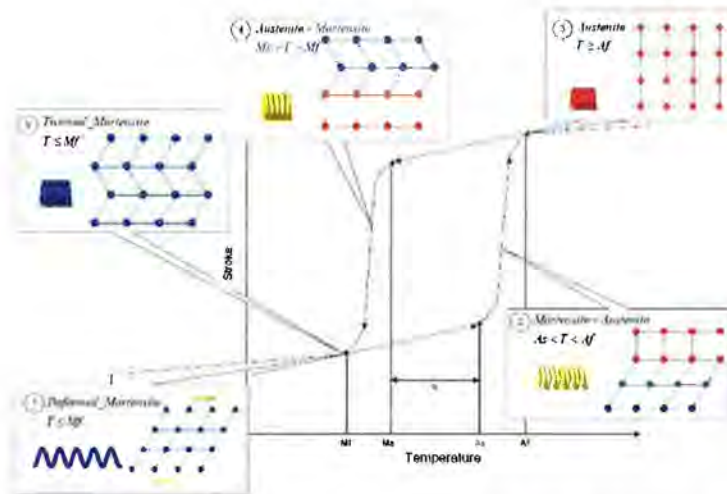


Figure 3: Shape Memory Alloys have two different solid states, which provides them their unique properties.

As shown in Figure 3, the first state, the Austenite state, occurs at relatively high temperatures. In this state the atoms of the SMA are in a rigid, crystalline lattice structure. It is in this state that the “preset” shape can be programmed into the SMA. The Martensite state occurs at lower temperatures, and in this

state the atoms are elastically held together in a structure that is the result of lattice twinning. As the metal cools below the Austenite state temperature it passes a transition temperature at which the atoms of the rigid, crystalline lattice begin to slide past each other. No bonds are broken in this transition; it is essentially a deformation of structure. Once below the transition temperature, the SMA can be deformed and bent. If it is heated to the transition temperature again, however, the bonds will shear, and align back into the rigid structure of the Austenite state, as shown in Figure 3¹⁴.

SMAs have long been applied for their unusual properties in a wide variety of situations. Their unique pliability and shape memory has rendered them excellent eyeglass frame materials. As braces wires, SMAs are able to exert a constant force over time across a multibracket braces system. The wire,



Figure 4: Examples of SMA stents.

which is deformed to fit a patients teeth as they are, tries to return to its Austenite shape once installed in the teeth brackets and exposed to the body heat. This motion exerts force on the teeth, which follow the movement of the

wire into proper alignment. Since nickel-titanium alloy SMAs have excellent biocompatibility, they have also been used as stents to repair blood flow through a vessel that has been blocked due to a condition like atherosclerotic deposits. In such a procedure, a compressed or “crimped” tube-shaped stent is inserted into a catheter and positioned in the blood stream. Since the transition temperature into the Austenite state (A_f) is lower than body temperature, as soon as the catheter is removed the tube expands to its programmed shape. This expansion pushes the vessel walls back, enlarging the channel. The stent will hold its shape, even if the vessel tries to contract again, because the temperature will always be above the temperature at which it would transition into the elastic, Martensite state. SMAs have also been exploited as staples or plates for bone fracture repair, and for many other uses in engineering industries¹⁵.

Project:

In this study a tracking mechanism was designed to increase solar panel efficiency. The project intended to optimize a system that could be applied to power a street light. The following is a discussion of the various aspects of the project, including the analysis and logic behind each piece of the design and testing of the efficiency of the design.

Choosing and Testing a Shape Memory Alloy:

After investigating different, readily available SMAs, nickel titanium alloys such as Nitinol and Flexinol® were settled on as the optimal materials for the tracking mechanism being designed. Capable of providing repeatable motion tens of millions of times when used within the technical guidelines, these alloys are designed to resist deformation caused by stress or strain¹⁶. Tests were run on 125, 250,

and 375 μm diameter Flexinol[®] wires and 750 μm diameter Nitinol springs to determine the percent contraction, pull force, heat of transition, and ideal load for each¹⁷.

SMA % Contraction vs. Mass Suspended		
Wire diameter (μm)	Mass (g)	Percent contraction (%)
125	115	4.28
	223*	4.98
	250	4.02
	300	4.86
250	105	8.00
	800	4.79
	895*	4.28
375	1565.2	3.67
	2065.1*	3.78
750 (spring)	200	57.5
	400	49.2
	600	47.2
	800*	44.6
	1000	41.6
	1200	36.8

Table 1.1: *Manufacturer recommended values

Analysis of the results (Table 1.1) showed that, while the thicker wires could achieve a greater pulling force than could springs before overheating, springs consistently produced a much higher percent contraction than the wires. In context, this greater contraction means that the spring will pull the weight over a longer distance when heated. With the goal of designing a rotor, springs were chosen as the ideal SMA shape. If wires were used, they would have to be much longer than a spring to pull the weight the same distance. Since compactness was an important element of the design, and springs were still capable of pulling ample weight, springs were chosen to drive the motor.

The Motor:

Initially in the motor design process the possibility of using a gear train to increase the torque produced by the springs was investigated, but while a potential mechanism was designed as discussed in

Appendix 2, it was found to be unnecessary and an overcomplication of what could be a fairly simple mechanism.

Springs had already been shown to be a more effective rotor than wires because they travel more under equivalent heat and mass load. Working off the idea of using SMA springs, the pieces that generally make up any kind of motor were investigated. A motor that causes movement of its load has 2 essential pieces: a stator and a rotor. The stator is stationary, anchoring piece that allows the rotor to “move” relative to it, and consequently move the load. The stator, then, cannot be influenced by the motion of either the rotor or the load, but must be connected such that these components have free relative movement. In the model of a solar tracking mechanism, the motion in question is rotation about a central axis. Since SMA springs were to be used to drive the motion of tracking they would be functioning as the rotor of the tracking motor. Thus, the SMAs and solar panel would need to have free rotation relative the stator anchoring the springs.

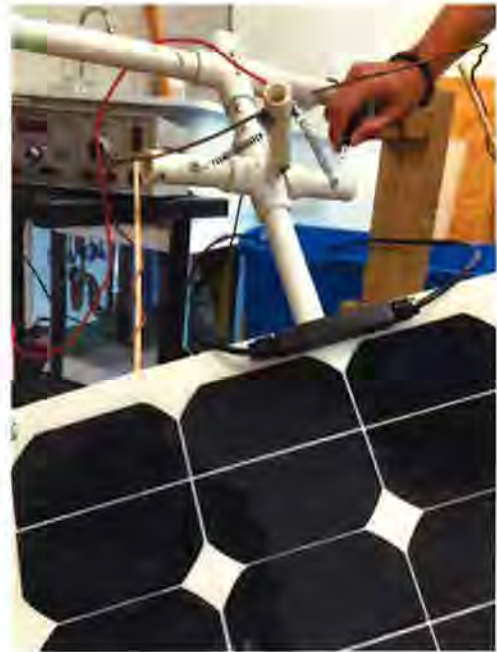


Figure 5: Mock-up of motor design being tested for strength when rotating the solar panel.

To accomplish this, a model of a tracker was designed and fabricated (Figure 5). The central axis supporting the solar panel from the underside was attached using U-brackets, so that the panel's rotation was not affected by the supports rotation. A stator was then built into the central axis (using PVC pipe in the model), so that the stator would also not be influenced by how the panel rotated. To drive solar panel rotation, springs were attached securely to either side of the front face of the stator, and the other end of the springs fastened to a perpendicular axis which had been affixed to the stator such that it could rotate side to side, parallel with the top of the solar panel (Figure 6).

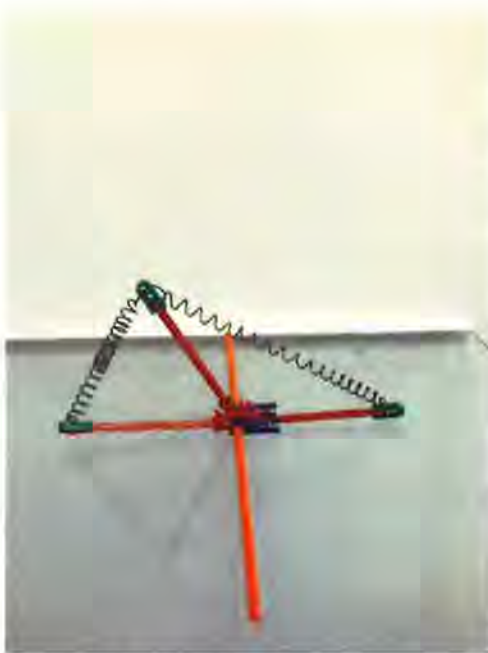


Figure 6: Model of proposed rotor design, showing SMA springs contracting and pulling a secondary axis toward the contraction.

A metal rod was next bent into shape, fed through this secondary axis, and then attached to the underside of the solar panel on each side of the center. In the model, wooden rods were used to increase the stiffness of the rotor-panel connection. While this would not be done in an actual build of the tracker, they were used in the model because the metal was too deformable to turn the panel without losing energy of rotation to deformation. In the final version of this mechanism, either a more suitable material would be acquired for the connection, or the principle of connection would be translated into a different configuration. These components provided the basis of

driving solar panel rotation. Figure 5 shows alligator clips being attached to one of the springs so that a current could be run through it, causing spring contraction. Testing the springs in this manner demonstrated that the system was sufficiently rigid to accurately rotate the solar panel.

In order for the springs to be deformed when the sun drove the system, however, there needed to be a way to exaggerate the directness with which the sun was incident on the springs as well as its intensity. To accomplish this, 2 lens would be installed on a casing surrounding the springs. The lenses would focus the incident light into a smaller but more intense ray on the springs. A style of lens called Fresnel lenses were chosen as they are inexpensive, durable, as they can be made from plastics, have short focal lengths, and can have focal lines rather than focal points. Two lenses would be set in openings in the top of the casing (Figure 7 only shows 1 lens), on the same plane as the face of the solar panel, and concentrate light onto one of both of the springs. An angle of the sun causing light to be incident on one lens more than the other would lead to contraction of one spring over the other, driving

contraction of the shape memory alloy metal, pulling the secondary axis in the direction of the contraction, and in turn rotating the solar panel toward the sun.

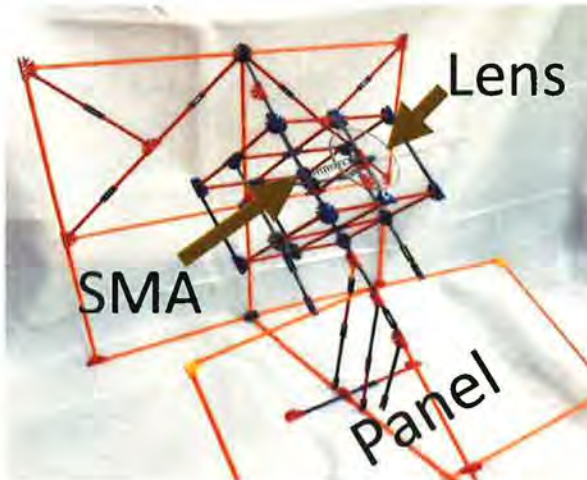


Figure 7: Model of proposed motor and solar panel system.

System Specifications:

A 50 W Sunpower, monocrystalline solar panel was purchased. The panel had a weight of 0.95 kg and measured 0.560 m x 0.540 m. To ensure the panel could be easily installed on a street light, and that it would last longer in any rough weather, a flexible, lightweight panel was chosen. A 12 V, 75 A·hr Mighty Max battery was purchased for the system. The 75 A·hr size was calculated to maintain a charge capacity above 50% when used without additional power input from the solar panel for 2 days, which could occur during a period of heavy cloud cover and low sunlight. Using the specifications of the



Figure 8: The solar panel set to the lowest of 3 settings on the stand is pointed toward the summer sun.

solar panel and battery as a guide, a Steca Solar Charge Controller was purchased to control the current into and out of the battery, and to protect against overcharging. The calculations used to determine the necessary specifications for each component are detailed in the next section.

It has been suggested that significant increase in the dual-axis efficiency has been seen with a clearness index of about 0.6. An index of about 0.4, however, does not provide a significant increase in efficiency⁹. The location of interest in this study (Arkadelphia, Arkansas, USA) has an average clearness index of about 0.5¹⁰. Because this value was below the suggested 60%, it was determined that a mechanical dual-axis tracker would not be worthwhile. However, as the value was not significantly below the recommendation, a manually-adjustable, north-south tracker was designed for the solar panel system, separate from the main, east-west tracker (*Figure 8*). This north-south tracker was designed to be adjusted seasonally. It consisted of a stand with a low height setting for summer, at which height the panel would be pointing more directly up in the sky, and a high height setting for winter, at which height the panel would be pointing more toward the southern horizon. A setting was also installed for fall and spring, which was in between the summer and winter heights. These height adjustments correlated roughly to the change in the zenith angle of the sun between the seasons. This system did not require much extra cost, did not add any maintenance costs, and added a bit of extra efficiency to the system. Calculations for these angles are presented in the next section.

System Calculations:

An 11 W flood light bulb was purchased as the model for the street light system.

Solar panel size^{18,19}:

$$[(\text{Watts of bulb} \times \text{hours of use}) / (\text{usable energy} \times \text{sun hours}) = \text{Watts of panel}]$$

$$(11 \text{ W} \times 14 \text{ hrs}) / (0.7 \times 3.88 \text{ hrs}) = 56.7 \text{ W panel}$$

Purchased a 0.95 kg, 50 W panel to allow for added efficiency due to tracking.

Calculations for battery size¹⁸:

$[(\text{Watt hours}/\text{Battery Voltage}) \times 2 \text{ days} \times 2 \text{ [keeps battery capacity over 50\%]}] = \text{Ampere hours}$

$(220 \text{ W}\cdot\text{hr}/12 \text{ V}) \times 2 \times 2 = 73.3 \text{ Amp hrs}$

Purchased a 12 V, 75 Amp hr battery

Calculations for the charge controller size²⁰:

$[(\text{Short-circuit current} \times \text{number of panels in parallel} \times \text{safety factor}) = \text{Amps of controller}]$

$(2.7 \text{ Amp} \times 1 \text{ panel} \times 1.25) = 3.375 \text{ Amp}$

Purchased a 12 V, 6 Amp charge controller

Calculations for the stand adjustment angles^{21,22}:

Summer angle = latitude \times 0.92 - 24.3° = 10°

Fall/Spring angle = latitude = 34°

Winter angle = latitude \times 0.89 + 24° = 58°

Efficiency Analysis:

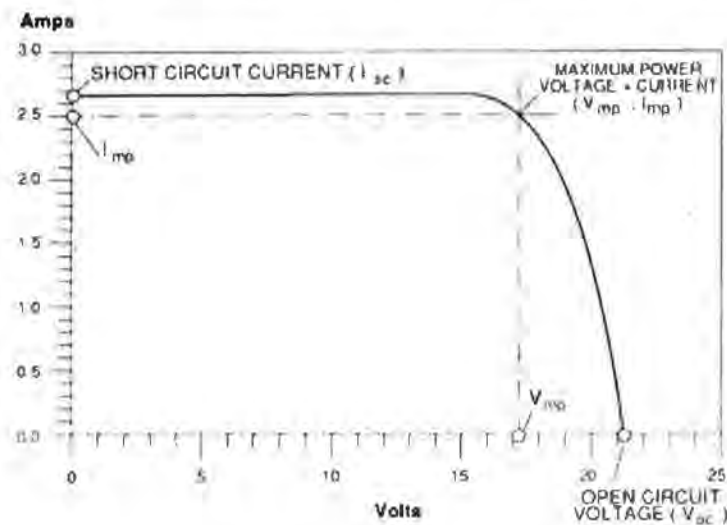
As would be expected intuitively, tracking has been shown to have the most efficiency gain compared to fixed panels during the parts of the day where the sun is farthest from its noon elevation⁵. This pattern emerges because, while a tracking solar panel is pointed at the sun all day, a fixed panel is only pointed directly at it around noon. Consequently, tracking and fixed panels align around the middle of the day, causing their efficiencies to converge, all other factors being equal.

In order to test the efficiency gain generated in the geographical region of interest to this study, Arkadelphia, Arkansas, data was taken using the solar panel to determine its maximum power output throughout the day on 2 different days. Both days chosen for testing were very sunny, and data sets were obtained at similar times on the 2 days. However, the days were separated by about 10 months.

This gap in time allowed us to examine the effects that the height of the sun above the south would have on efficiency. The data sets were taken in June and April. The average clearness indexes for the general area in June and April are nearly identical (0.56 and 0.55 respectively), but the angle of the sun above the south is higher in June than in April ¹⁰.

Maximum power output at each time was calculated by recording the voltage and current generated by the solar panel when passed through resistors of varying values. Higher resistance yields lower current (measured in Amps) and higher voltage (measured in Volts), while lower resistance yields higher current and lower voltage. Power is equal to the product of voltage and current, so by multiplying these together for each individual resistance value the power output is given. Comparing the power values together within each time slot, the maximum power output value for that was found. On an ideal current vs. voltage plot, this point can be found at the bend of the plots curve (Figure 9).

Figure 9: Ideal Current (Amps) vs. Voltage (Volts) plot, showing maximum power at the peak of the curve.



The process of passing the solar panel current through a series of resistors to determine power was repeated a minimum of 3 times on each day in both a fixed configuration and a tracking configuration. A tracking configuration simply mimicked the action of a solar tracker by manually tilting

the panel to an angle such that its surface was directly in line with the sun. The parallel times from data sets #1 and #2 were compared, as were the overall values within each data set. Data set #1 was taken on June 26th, 2018. Data set #2 was taken on April 10th, 2019. Raw data for each data set is attached in Appendix 3, and detailed instructions for collecting efficiency data are available in Appendix 2.

Table 1.2 details the average percent difference between the fixed and tilted maximum power output values for each comparable time slot across the data sets. As expected, the difference between them is much greater as the times get farther from noon. Closer to noon (1 PM), however, the percent difference is negligible. The average percent difference calculated across the different times, 62.77%, is expectedly high. The typically reported percent efficiency increase for tracking compared to fixed solar panel systems is ~40%⁵. Such values, however, are more inclusive of long periods of time and variances in weather and time of year. The data obtained in this study intended to show whether tracking provided a significant increase in power in the geographical region of interest, but was not intended to be an all-inclusive determination of what the average relative efficiency might look like. *Table 1.3* compares the increase max power and the percent increase in max power compared to the fixed panel for both data sets. Consistent with the average values, the trend of increased power output relative to fixed panels holds throughout each day, and between the data sets, indicating the trend is not season specific. Thus, from this data it was concluded that tracking is beneficial for efficiency in this area, regardless of the dips in efficiency that will be experienced on days that are less clear and sunny.

Time	Average % Difference
10:00 AM	74.95
1:00 PM	6.31
6:00 PM*	107.04
Average	62.77

*Table 1.2: Averages of sets #1 and #2. *6:00 PM value is an average. Actual times were #1: 6:30; #2: 5:30. While different, the times are compared because they are both ~2 hrs before sunset on the day of interest (#1: 8:28 PM; #2: 7:40 PM).*

Set #1: June 26 th , 2018			Set #2: April 10 th , 2019		
Time	Max Power % Increase	Max Power Increase (Watts)	Time	Max Power % Increase	Max Power Increase (Watts)
10:00 AM	35.24	7.59	10:00 AM	299.64	18.27
1:00 PM	6.73	1.91	1:00 PM	6.31	1.66
4:30 PM	49.75	9.9	5:30 PM	245.36	12.86
6:30 PM	216.2	13.38			

Table 1.3: Comparison of data sets #1 and #2, demonstrating the consistent trend of increased power output relative to fixed panels throughout the day, and at different times of year.

One time slot within data set #2 (5:30 PM) did suffer some minimal but consistent cloud cover. The time was such that the tracking configuration turned the panel 45 degrees toward the west compared to the fixed panel. Comparing the efficiency data gathered from this time slot with the corresponding time slot in data set #1 showed that, while the clouds did reduce power output, tracking still increased maximum power output relative to the fixed panel by 245.36%, with a 110.19% difference between the fixed maximum power and the tilted maximum power, and a 12.86 Watt increase in power (Table 1.4)

Time (PM)	P (fixed) (Watts)	P (tilted) (Watts)	Percent Difference	Percent increase in max power output	Watt increase
5:30	5.2432	18.108	110.1853	245.3616	12.8648
6:30	6.187	19.5636	103.8935	216.2049	13.3766

Table 1.4: Comparison of light clouds (5:30 PM) with sun (6:30 PM). While different, the times are compared because they are both ~2 hrs before sunset on the day of interest.

Results:

Solar energy is a valuable power source that can be harnessed with relative ease. The important issue in developing the industry and working sustainable energy into the mainstream is efficiency. By designing mechanisms that increase the power output of a given solar panel system and tailoring them to their intended application and geographical area, solar energy can become more efficient, cost effective, and accessible.

Intent on designing a motor that would rotate a solar panel in line with the movement of the sun throughout the day, and a system that would be easily implemented in a remote area to power a system such as a street light, a model mechanism was fabricated using shape memory alloy springs as rotors. The system, classified as a passive tracker, was shown through testing to increase efficiency by an average of 62.77% on sunny days, thus providing a significant power increase. It was also shown to be effective at increasing the current from incident sunlight under mildly cloudy conditions. While the motor and solar panel system require further refinement before being applied to real-world systems, a framework has now been developed from which future design work can grow.

Appendix 1: Efficiency Data Instruction Manual

The following is an instructional guide for collecting efficiency data from the solar panel system.

While initially written to walk work-study or research students through the process if more data

were needed in future research, the manual's instructions may differ slightly from the

procedure that was finally followed in collection of the referenced data. However, it is still

included here as a guideline.

PROCEDURE FOR SOLAR PANEL VOLTAGE/CURRENT DATA COLLECTION

Introduction:

You will be helping collect data for Dr. Douglass's solar tracking research. After initial setup, this will consist of logging voltage and current data given off by a solar panel that is set up in 2 different orientations.

You will collect the data in spreadsheets. Please send these to me (Keeley Johnson: joh60996@obu.edu) as you fill them out. Also don't hesitate to contact me with questions or problems that come up!

We will need 30 sets of data from 3 different time slots, for a total of 10 sets from the mornings, 10 from the early afternoons, and 10 from the evenings. The values recorded will help us understand the power output of the solar panel, and the effect of turning the panel directly toward the sun during data collection, compared to keeping it in a fixed position.

Materials:

5 alligator clips

2 voltmeters

Cords for voltmeters (2 black and 2 red)

Solar panel

Solar panel stand

Decade resistor box

Excel

Website for solar angle measurement:

https://www.sunearthtools.com/dp/tools/pos_sun.php?lang=en#txtSun_2

Procedure:

1. Initial setup: includes the setup of the electronics that will be the same throughout the experiment. You can keep it set up from day to day, but make sure the voltmeters are turned off, and unclip and move one of the solar panel cords, so that the exposed end won't touch any of the other metal parts.
 - a. Clip an alligator clip to the solar panel's "+"-labeled cord on the exposed wire.
 - b. Clip the other end to the decade resistor box, on the top of the input knob.
 - c. Turn the X100K dial to 10.
 - d. Connect a 2nd alligator clip to the base of the same knob.
 - e. Clip the other end to the red cord of a voltmeter (referred to as **voltmeter 1**).
 - f. Make sure the dial of the voltmeter is set to off.
 - g. Clip a 3rd alligator clip to the black cord of the voltmeter.
 - h. Clip that clip to the base of the other knob.

- i. Use a 4th clip from the top of the 2nd knob to the red cord of a 2nd voltmeter (referred to as **voltmeter 2**).
- j. Make sure the dial of the voltmeter is set to off.
- k. Clip a 5th from the other cord of the voltmeter to the exposed wire on the “-”-labeled cord of the solar panel.



Step a: alligator clip on (+) wire



Step b, d, h, and i



Step c: decade resistor box

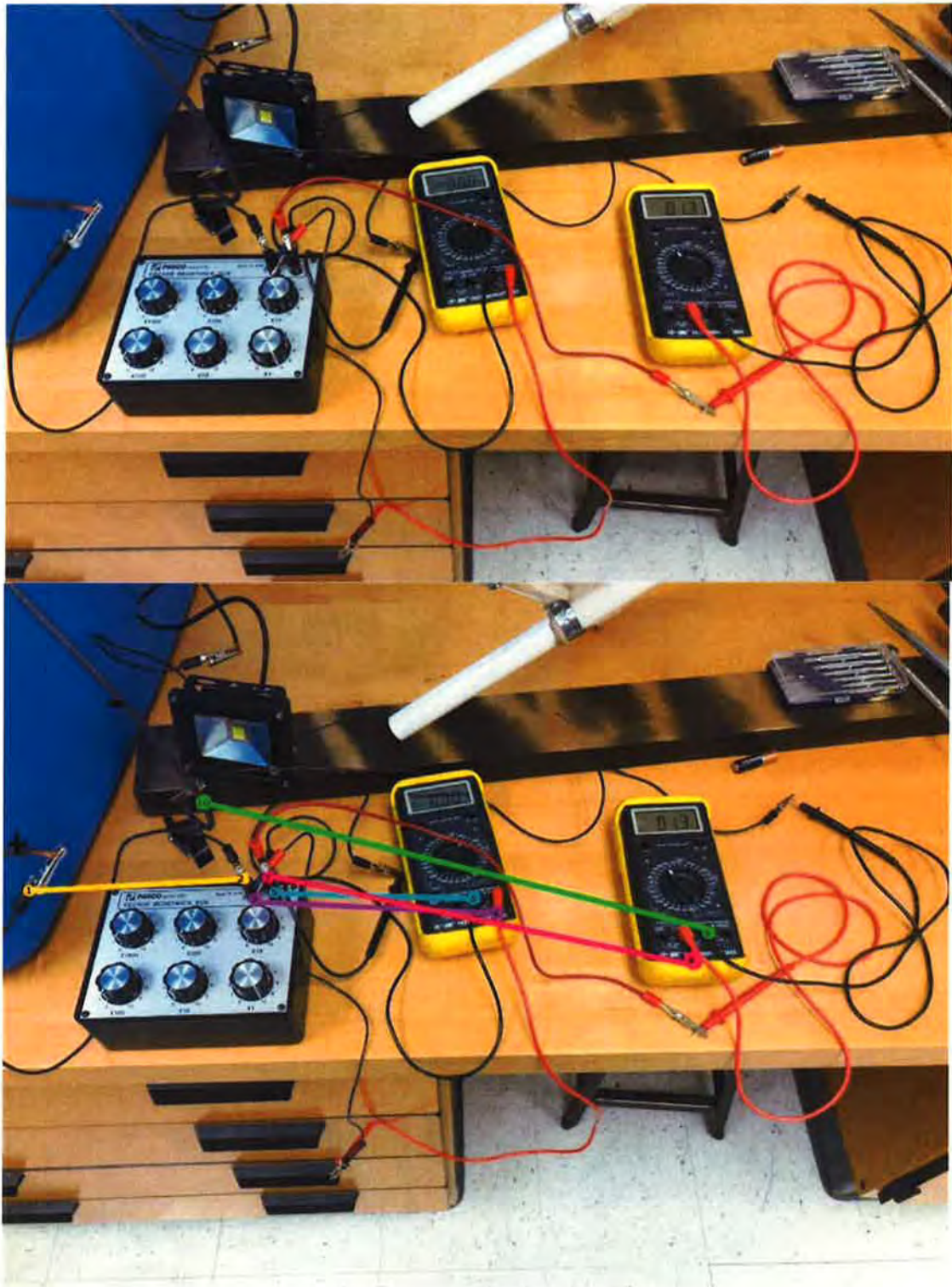


Make sure the red and black cords are plugged into voltmeter 1 as shown.



Make sure the red and black cords are plugged into voltmeter 2 as shown.

- i. Glue/drill a meter stick or some other long, stiff, straight-edged object to the base of the panel stand such that one edge intersects the center of the axis of the solar panel. Use this as a center line when measuring angles with a protractor later.



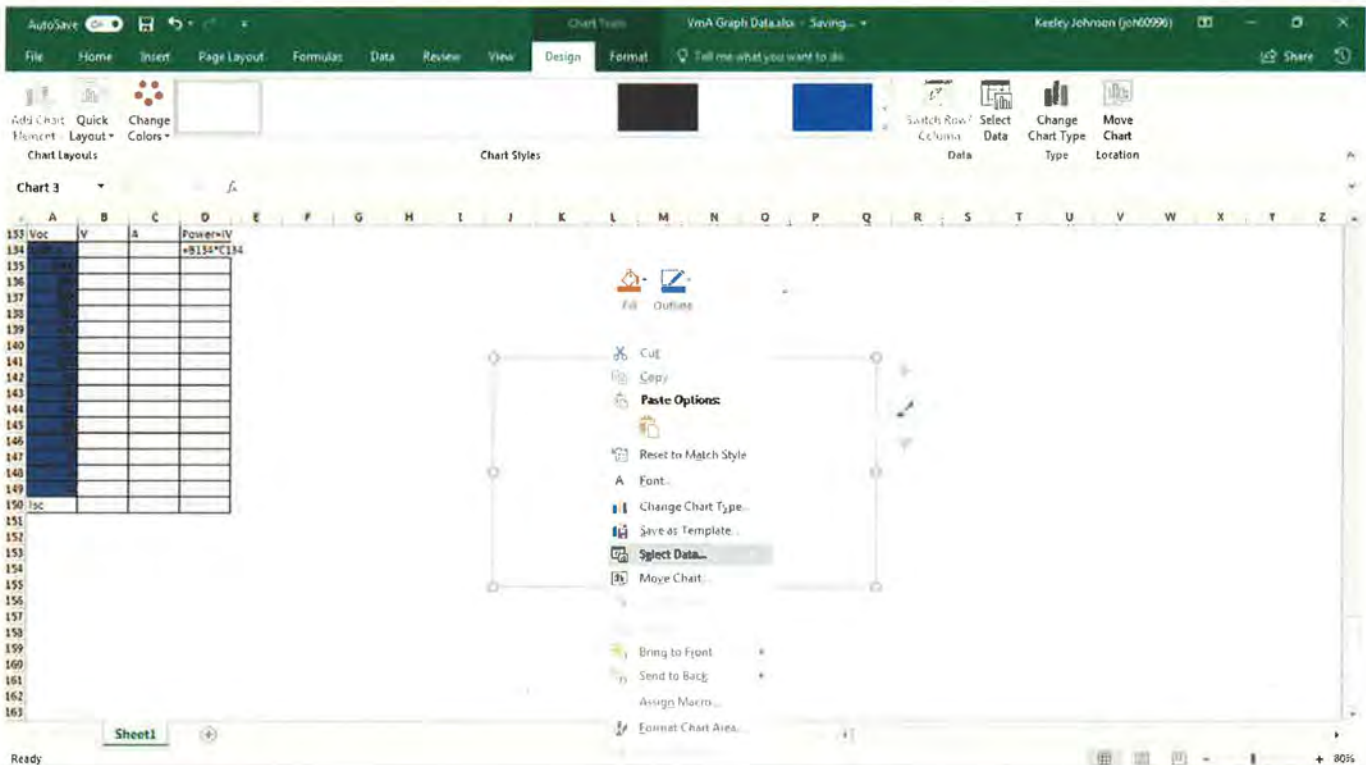
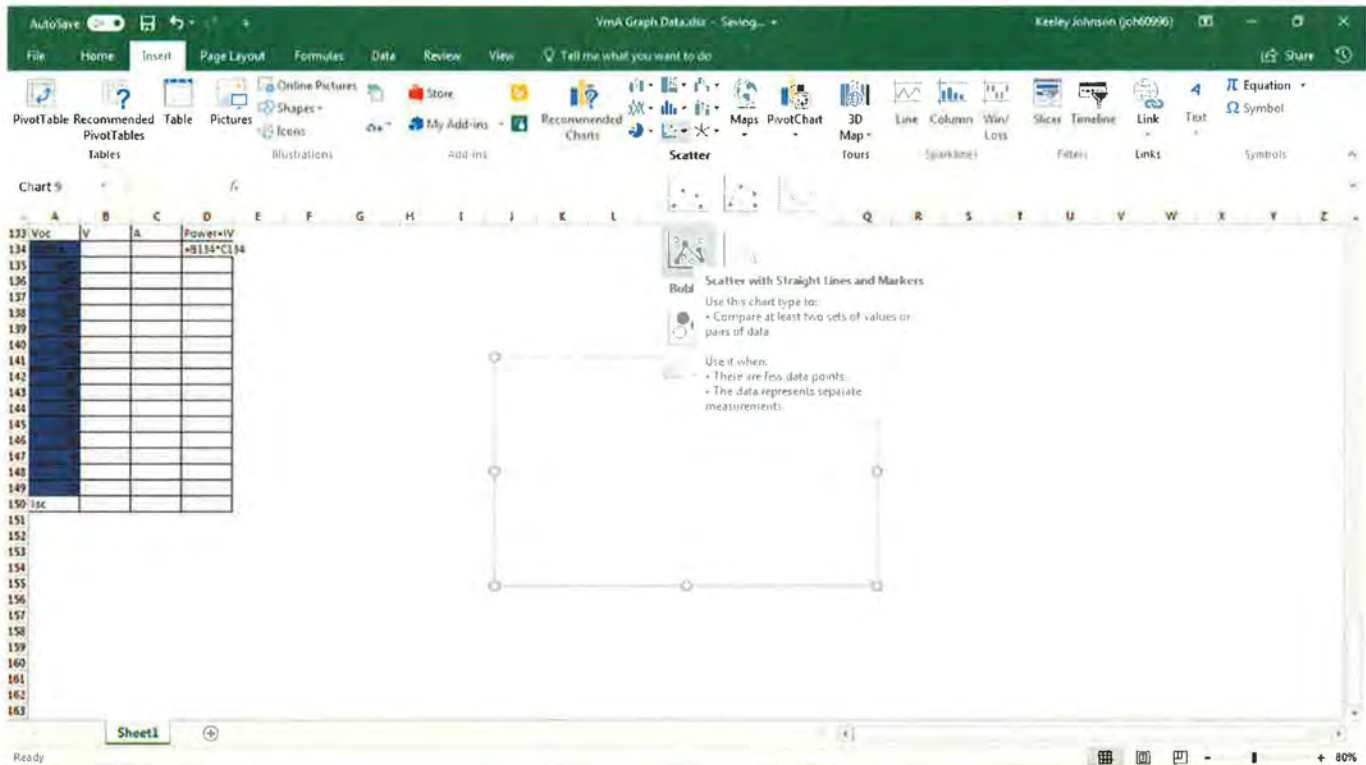
Yellow: step a-b. Purple: step d-e. Blue: step g-h. Pink: step i. Green: step k. In the figure, voltmeters are not set to off. Make sure they are off when setting up. Voltmeter 1, on the left, will measure voltage (volts). Voltmeter 2, on the right, will measure Current (amps).

2. Logging data

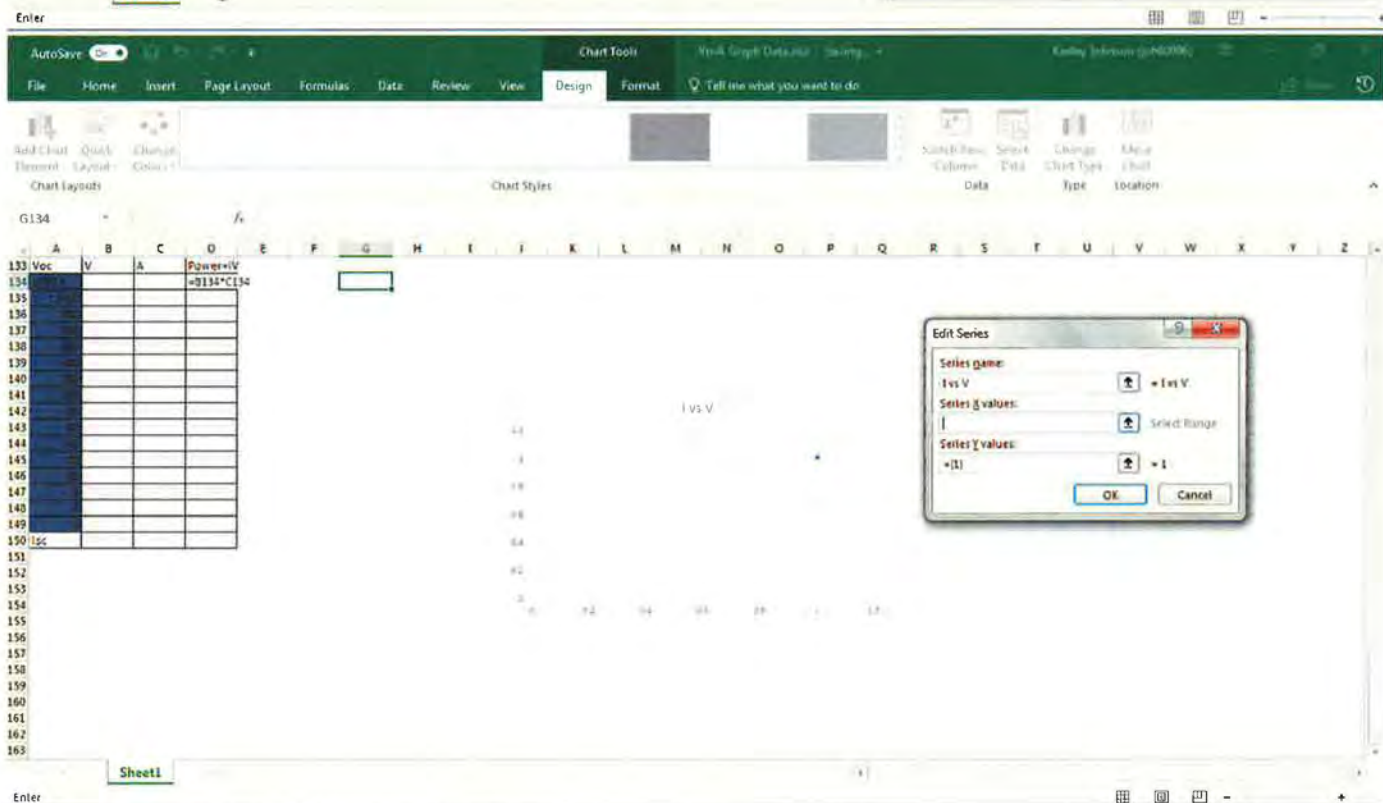
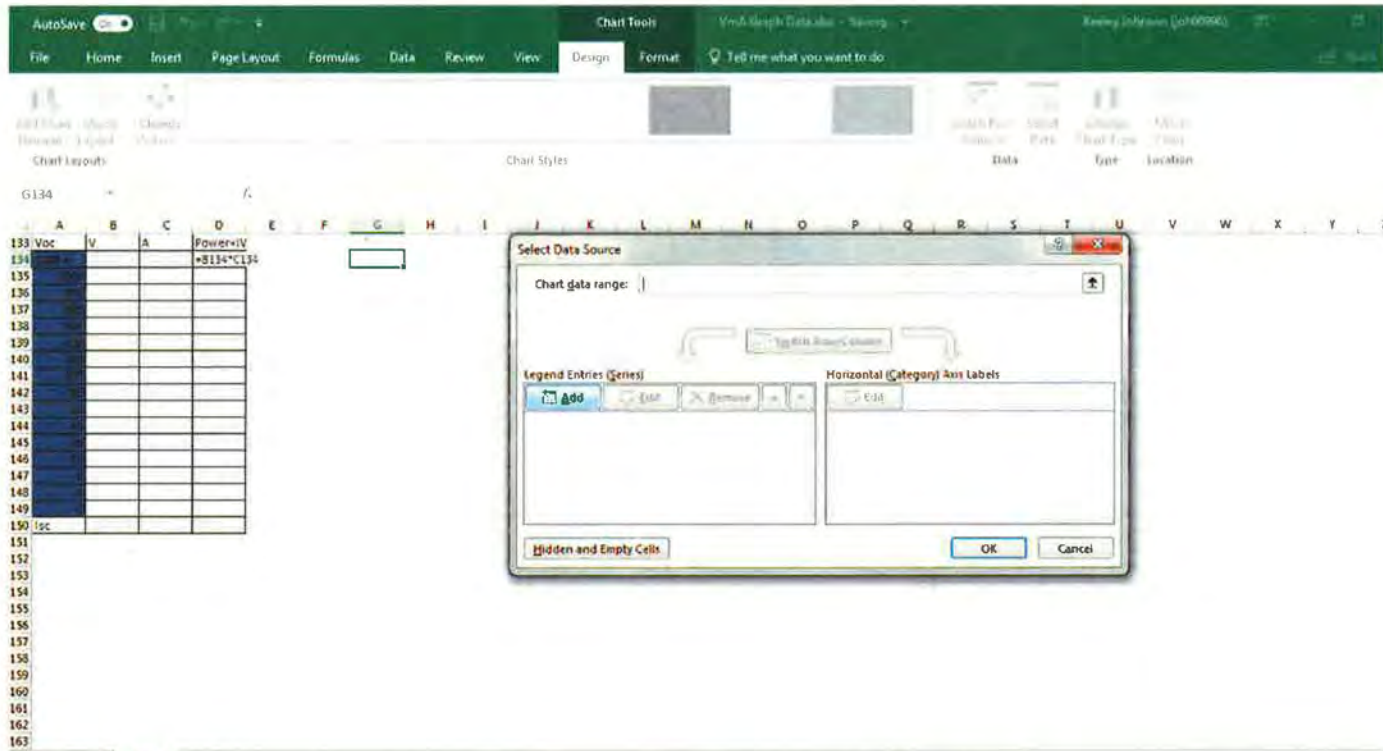
- a. Spreadsheet: I've made a template spreadsheet, but this section gives directions on recreating it if necessary.
 - i. Label columns, as shown, V_{oc} (Voltage open current), V (voltage in Volts), A (current in Amps), and Power=IV. Label rows in the increments indicated.

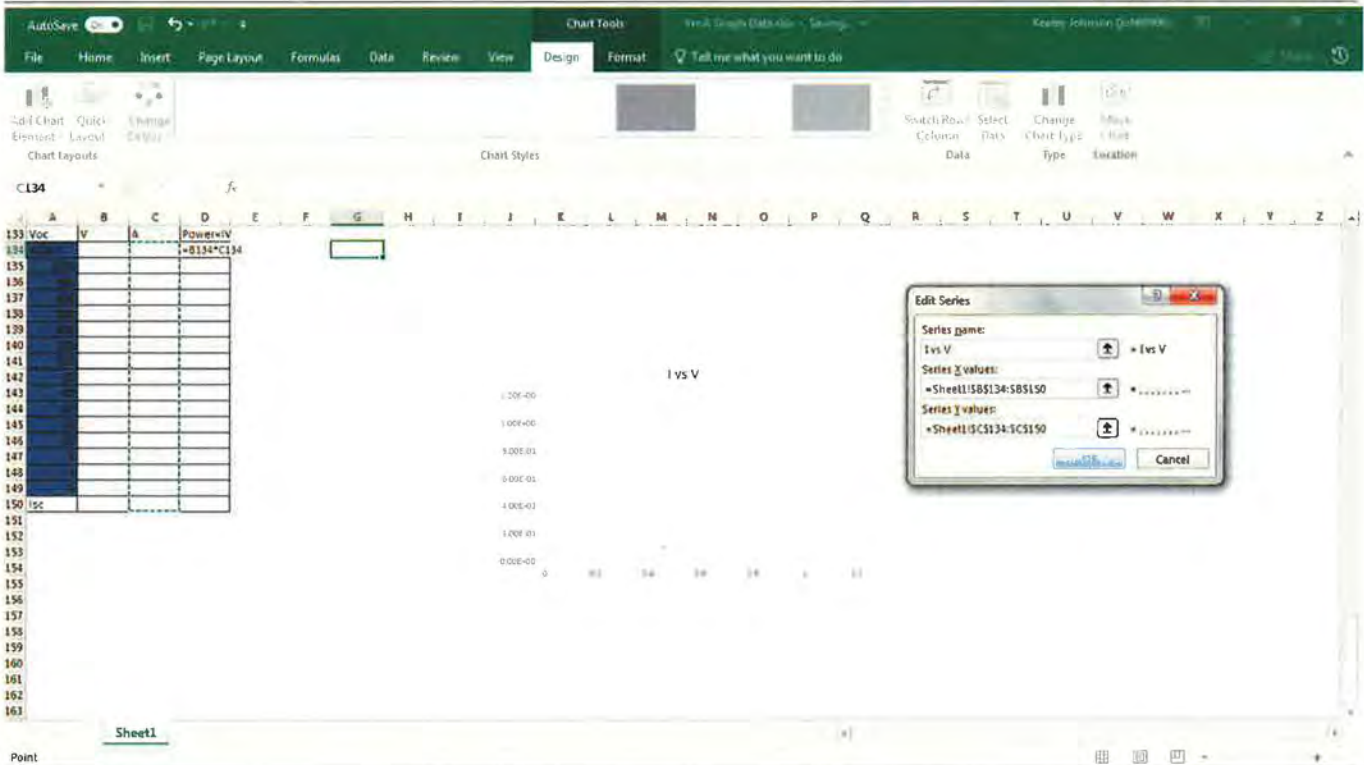
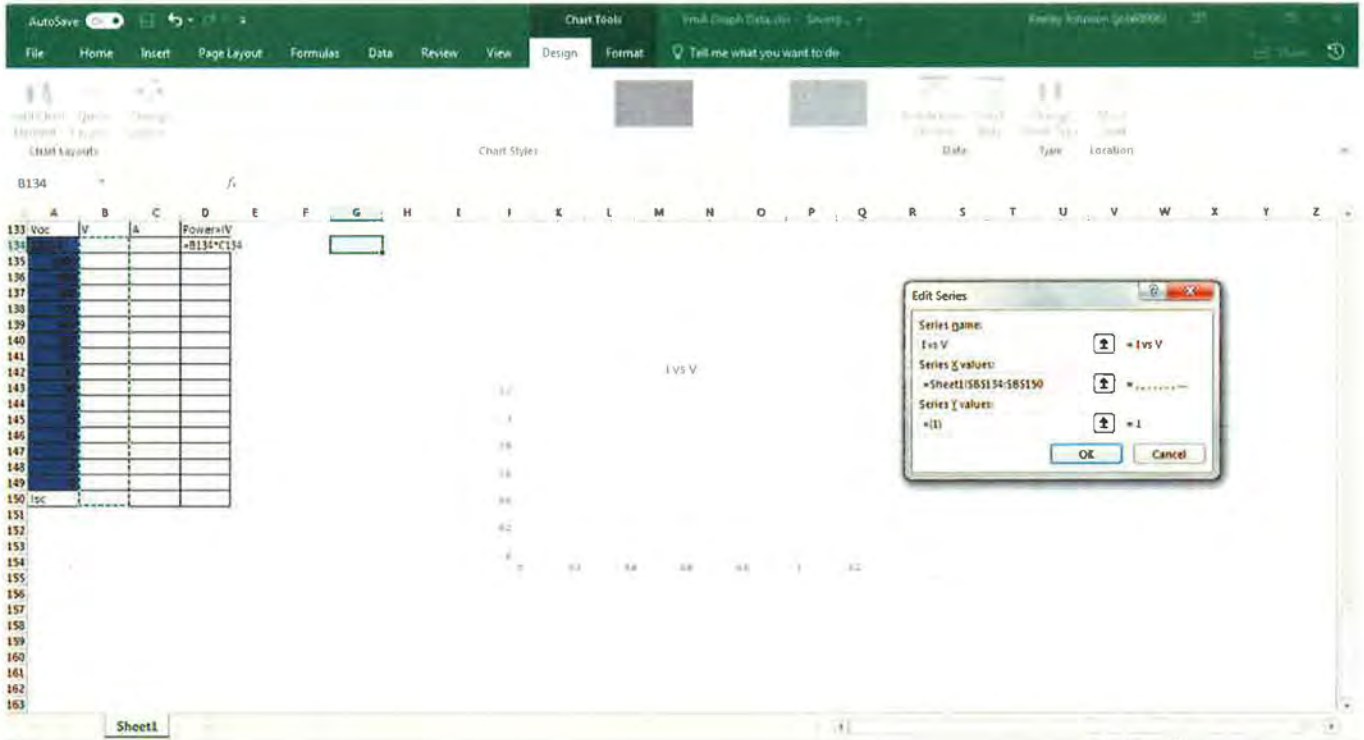
Voc	V	A	Power=IV
1000 V			=B134*C134
900			
800			
700			
600			
500			
400			
300			
200			
100			
0			
Isc			

ii. Insert a scatter-plot graph

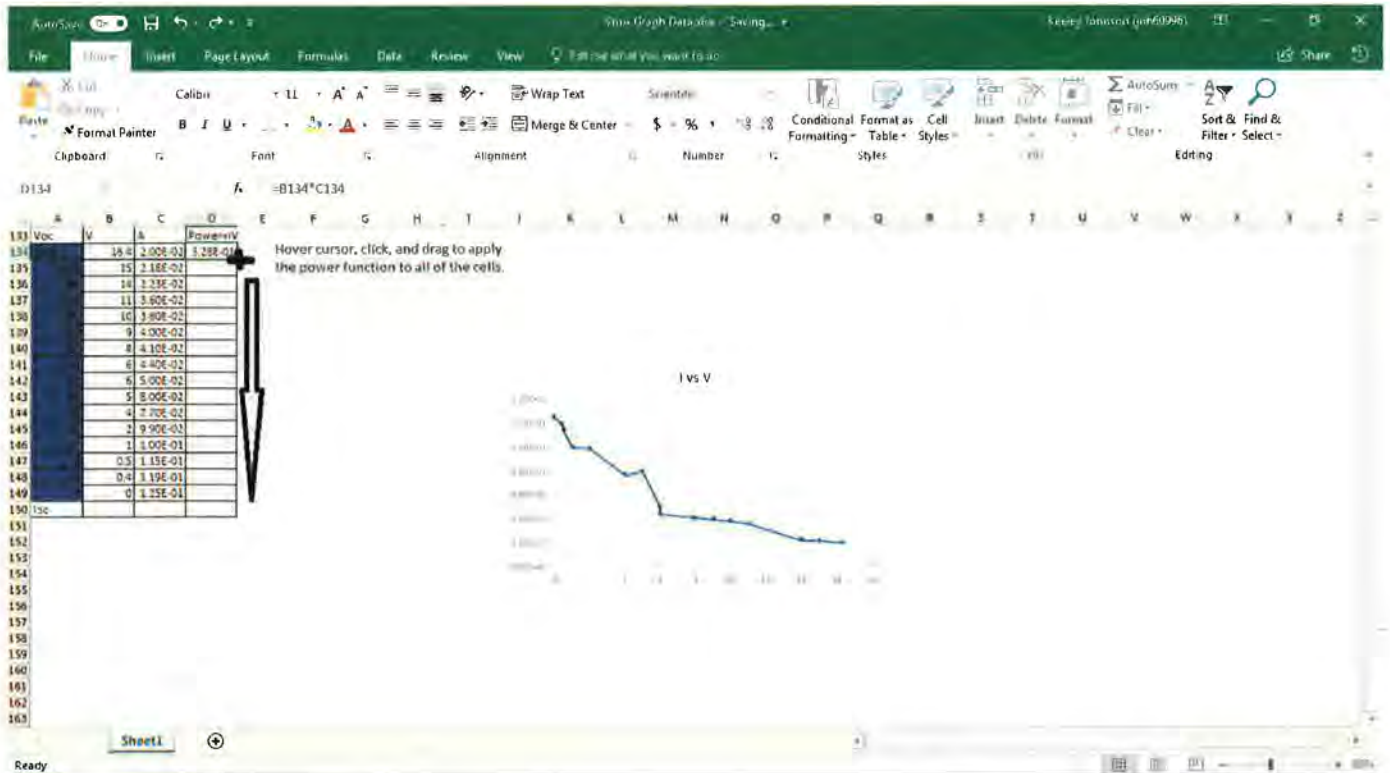


iii. Select column V as the x-data set and column A as the y-data set.





- iv. Set the Power=IV cells equal to the product of the V and A cells adjacent to it (on the same row).



- b. Using the voltmeters, and acquiring/formatting individual data points:
- Turn the X100K knob on the decade resistor box to 10.
 - Turn the dial on voltmeter 1 to 40 V.
 - Turn the dial on voltmeter 2 to 400 μA .
 - Allow displayed numbers on both voltmeters to settle as much as possible before recording the values. Some shifting may be present, in which case record the best average you can.
 - Record the values from voltmeter 1 in the V column, and the values from voltmeter 2 in the A column. Make sure to convert μA to A (on a spreadsheet, enter for example 16.5e-5 instead of either 16.5 or .0000165. It just makes life easier, not having to do the conversions).
 - Save the spreadsheet files in the format "Monthdayyear-time of day-solardatacollection.xlsx" For example, 012818-morning-solardatacollection.xlsx
 - Vary the resistor box knob settings as directed in the procedure.
 - If a voltmeter reads "**overload**," turn the dial up one setting at a time until it displays a number again. This may change the units of the value. If you don't understand the change, ask Dr. Douglass or myself. The markings indicate the highest value the setting can handle, and the units it is displayed in. The μA dial will almost definitely need to be turned up, but when depends on the amount of sunlight present.

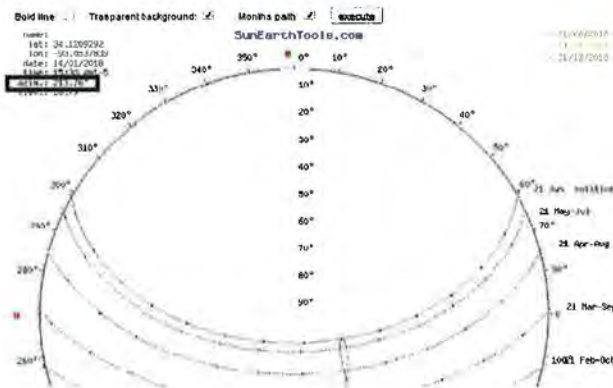
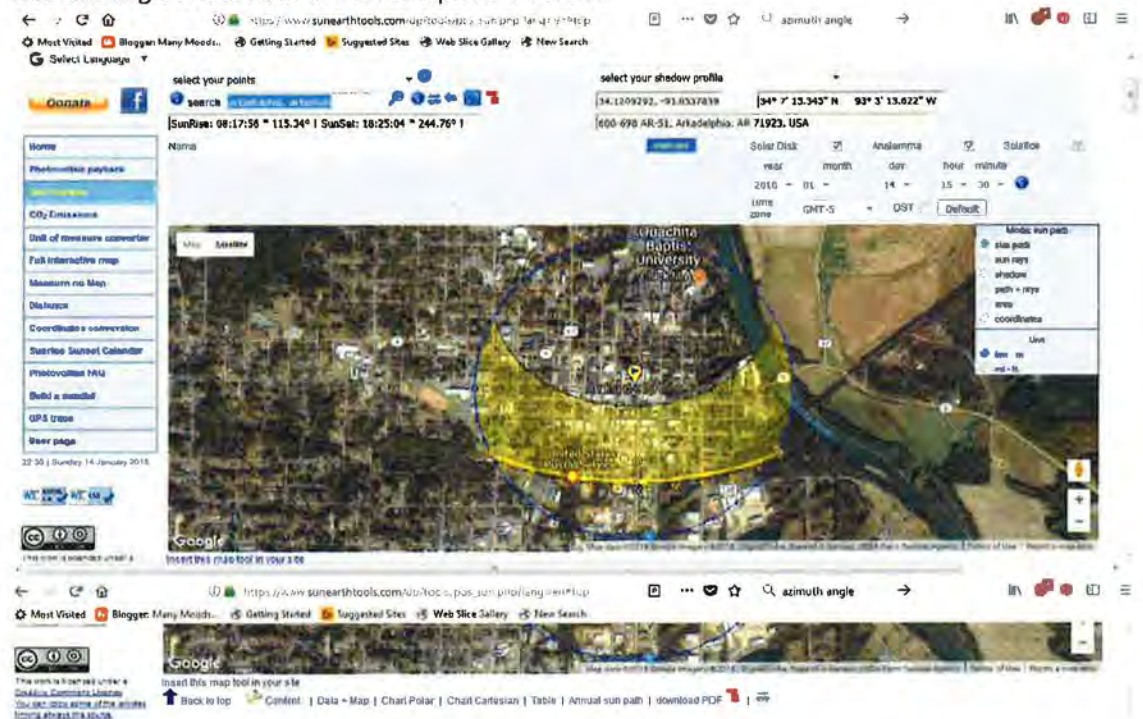
- ix. If a voltmeter starts **beeping**, turn it off, and check the connections and settings.
- x. To measure the angle of the solar panel to the earth, align the straight edge of a protractor approximately with the edge of the solar panel, and read the angle indicated by the centered straight edge. When the panel and the sun are in line, adding 90° to that measurement gives the azimuth angle of the sun, or the angle of the sun across the sky. The azimuth angle should always be between 90° and 270° .

3. Collecting Data

a. Find the azimuth angle from:

https://www.sunearthtools.com/dp/tools/pos_sun.php?lang=en#txtSun_2

Scroll to the top of the page, inputting "Arkadelphia, Arkansas" in the search bar. Make sure that the current time is displayed, or adjust the time/time zone accordingly. The azimuth angle is boxed in the second picture below.



- b. Take the solar panel, stand, connected wires, resistor box, and voltmeter out to the loading dock.
- c. Place in as full sun as possible, facing away from the science building (south).
- d. If it is winter, hook the panel on the top rung of the stand. If it is spring or fall, hook it on the middle rung. If it is summer, hook it on the bottom rung.
- e. Make a note of the weather conditions somewhere to the side on the spreadsheet.
- f. Rotate the panel such that the face is parallel to the ground (read 90° on the protractor)
- g. Make sure the wires are all connected as directed in step 1.
- h. Read the V (voltage) and A (current) values at 1000K (=10 on the 100K dial) as indicated in 2b, logging the numbers in the spreadsheet's appropriate columns on the 1000K row.
- i. Turn the X100 knob to 10. Turn the X100K knob to 0. Follow the same procedure to take V and A values at this resistance setting.
- j. Repeat for all rows in the spreadsheet, using the X10 knob for 10-100, and the X1 knob for the single digits.
- k. Save the spreadsheet, indicating it is the FIXED data set.
- l. Turn the panel to the azimuth angle. To align the panel with the sun, subtract 90 from the azimuth angle given on the site, and turn the solar panel to the new angle. The panel should be directly in line with the sun when done properly. If it is obviously not, check time zone, and that the protractor has been used properly.
- m. Record the data from parts h-j for the new angle on an identical spreadsheet setup. Save the spreadsheet, indicating it is the Azimuth data.

Appendix 2: A Discussion of Gear Trains and Inquiry into their Applications for Solar

Tracking Motors

After deciding to passively track with shape memory alloys, the question of torque was addressed. While the SMA springs would be capable of producing some torque on the solar panel during contraction, it was unclear whether they would be strong enough to rotate the panel with the required range of motion. Further, the potential for wind or other elements to damage the panel or motor by violently turning it against its tracking position was concerning. For these reasons the possibility and practicality of employing a gear train in the motor was considered. Although finally rejected as not providing enough benefit to outweigh the added cost, upkeep, space, and difficulty of construction, the resulting designs and applications may be of interest to readers.

A gear train is a system of multiple gears that fit together and by being driven at the beginning of the train act to on some target at the end of the train. Gears may be driven by steam, in the context of a steam powered turbine for example, driven by computerized mechanisms, motion of some other area such as a wheel, or in this theoretical application, the motion of contracting SMAs. The points around the circumference of a gear are called "teeth;" the distance from the beginning of one tooth to the next is the "pitch;" the length of the tooth (equally the depth of the groove between the teeth) is the working depth, or clearance; the diameter of the gears central hole is the "bore." In order for 2 gears to mesh their pitches must be equal²³.

To successfully track the sun, the panel needed to have a range of at least 90° , or $\pm 45^\circ$ from the center. While still in the process of testing SMAs and designing the motor, it was unclear whether they would be capable of producing the torque necessary to rotate the 0.95 kg panel. Torque can be adjusted from its essential level by varying the radius of gears, and thereby the number of teeth, in a gear train. By beginning with a small gear with few teeth and using that gear to drive a larger one with

more teeth, torque is increased. Relative torque can be calculated from the gear ratio between two gears. The gear ratio represents the ratio of the number of teeth of the driven gear to the driving gear. For example, if a gear has 10 teeth total on its circumference and is driving a gear with 60 teeth, the gear ratio between them is 4:1, and the relative torque is 4. If however the gears are reversed, with 60 teeth driving 10 teeth, the ratio is 1:4, and the relative torque is $\frac{1}{4}$. Thus, to ensure torque was increased relative to the initial force produced by the SMAs the gear train would need at some point to have a large gear ratio.

A Worm gear (*Figure 10*) is typically a rod shaped, rather than circular, gear. Due to its unique teeth structure it is only capable of driving a paired gear in one direction. Rotation of the worm gear, say to the right, will push the paired gear forward and rotate that gear. Rotation of the worm gear to the left, however, will have no effect on the paired gear. The worm gear will continue to rotate as long as driven to do so without disturbing the other gear at all. Because of concerns regarding potentially damaging back-turning of the solar panel, including a worm gear in the mechanism was a logical protection against losing current due to back-turning, or damaging the solar panel system²⁴.



Figure 10: Several styles of worm gear.

When a gear drives another gear, the direction of rotation between them is reversed. Thus, in order to ensure that SMA contraction drove the gear train to turn the solar panel toward the direction of contraction, an even number of gears had to

be used. Including the worm gear that number, an odd number of other gears had to be used.

In the process of designing the gear train, the need for gears to turn right angles was unavoidable. Bevel gears are angled at 45° on their teeth, and by meshing together form a right angle.

Mitre gears are pairs of beveled gears that have the same numbers of teeth. Using these allows the angle adjustment necessary, without changing torque or ratios²⁵.

While a gear train was designed that could potentially address the concerns it intended to, through research into manufacturing companies and suppliers it was found that specific size and tooth number availability was relatively limited on small scale gears. This difficulty set limits as to how small the gear train could be, an issue not easily reconcilable with the intent of the design. For the solar panel system of interest, the motor needed to be low profile and easily maintained. Further, testing of SMA springs showed that the torque they produced would be capable of adequately driving the solar panel rotation. With the increased complexity of a gear train, the necessity for it to be larger than designed which would contribute to unwanted bulk in the system, and the knowledge that gears would wear out and corrode more quickly than the other parts of the motor, it was determined that the potential benefits granted by a gear train were not outweighed for this system by the issues²⁶.

Figures 11-13 show a 3 dimensional model built on the program Autodesk Inventor® of the gear train design. It is composed of a worm gear which would be rotated by SMA contraction driving a pinion (or small) gear compounded with a larger bevel gear. Compound gears are attached and aligned such that turning one causes the other to turn. It is beneficial in this system because it allows a rapid increase in size of gear while using as few gears as possible. This bevel gear rotates a second bevel gear which is fixed to the casing of the motor, and by turning the casing the whole panel is turned. This section of the motor, which does not include the casing, springs, or central axis attaching the mechanism to the solar panel is approximately 4" x 5" x 4.5".

Assembly.iam



AUTODESK VIEWER

Figure 11

Assembly.iam



AUTODESK

AUTODESK VIEWER

AUTODESK

Figure 12



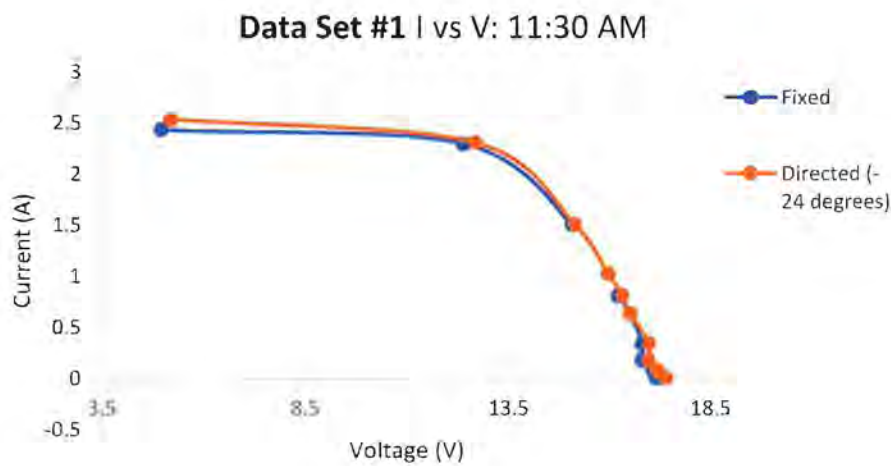
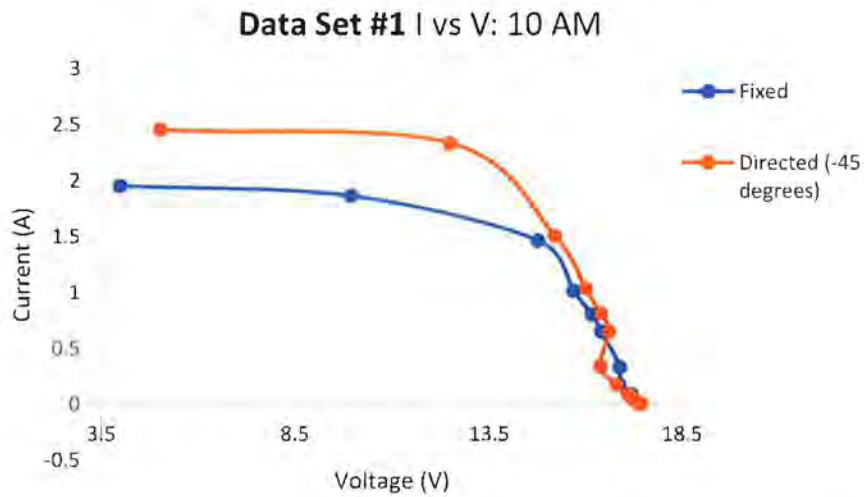
AUTODESK VIEWER

AUTODESK

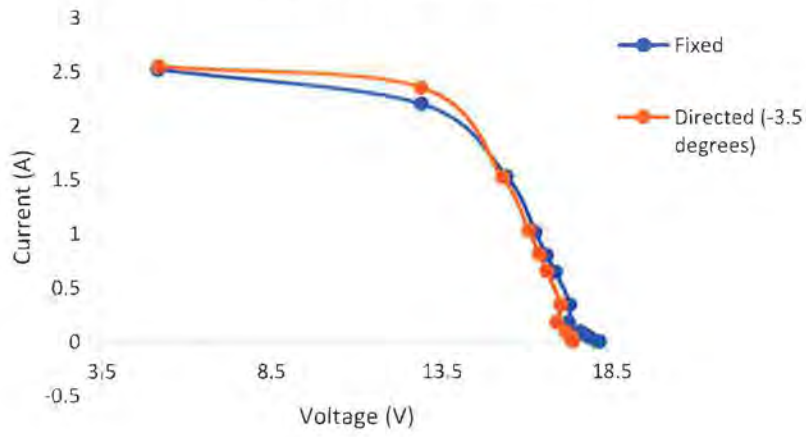
Figure 13

Appendix 3: Efficiency Data

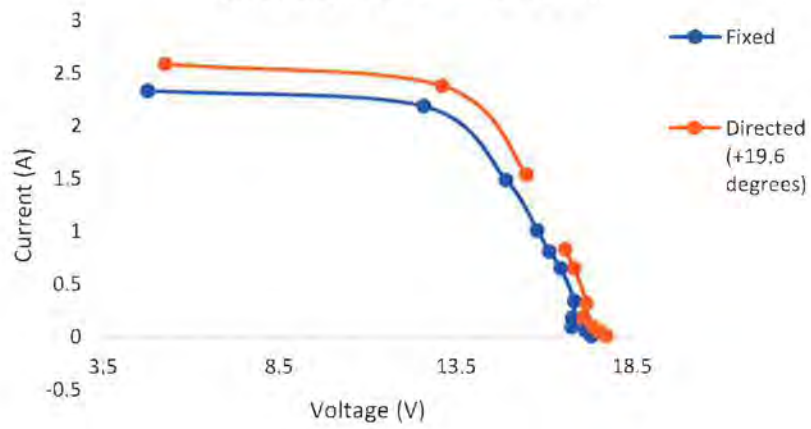
Current vs. Voltage graphs for each time slot of data taken, including both Data Set #1 (June 26th, 2018) and Data Set #2 (April 10th, 2019). Time of measurement and angle of direction are indicated on the graph.

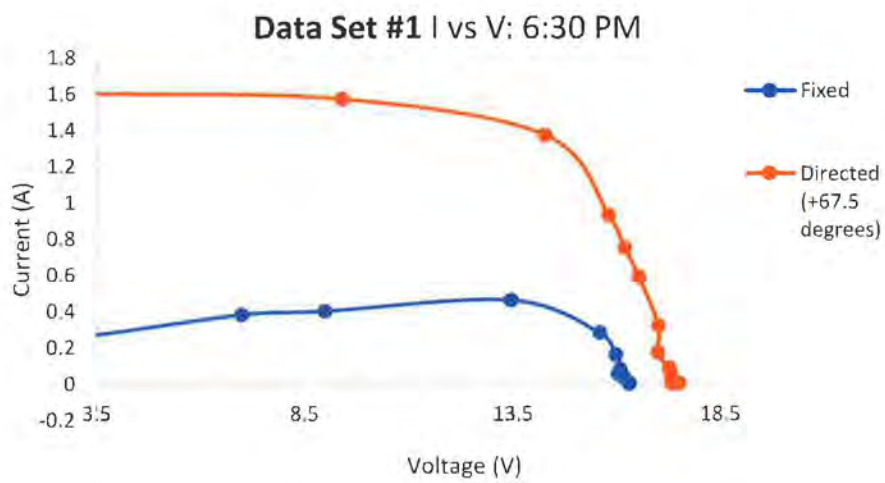
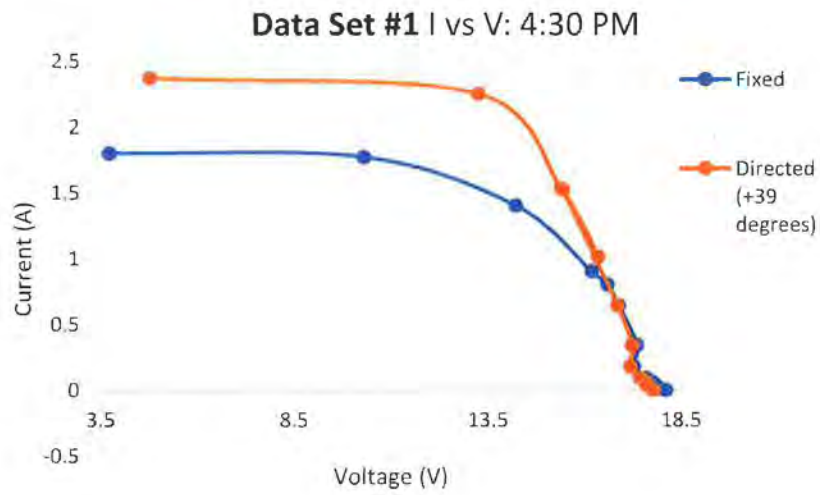


Data Set #1 | vs V: 1 PM

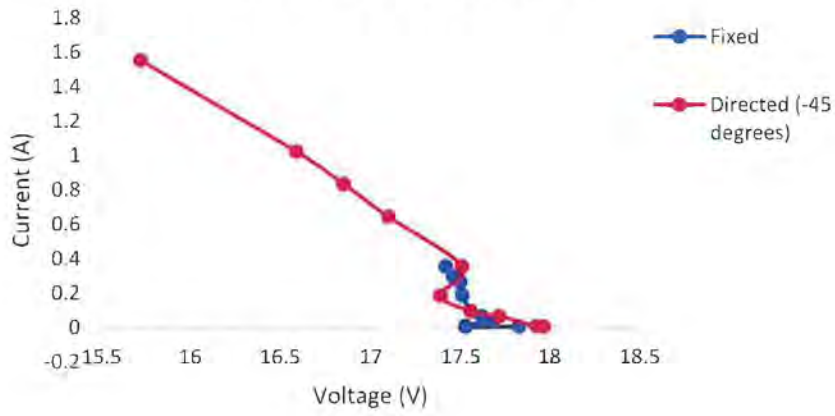


Data Set #1 | vs V: 2:45 PM

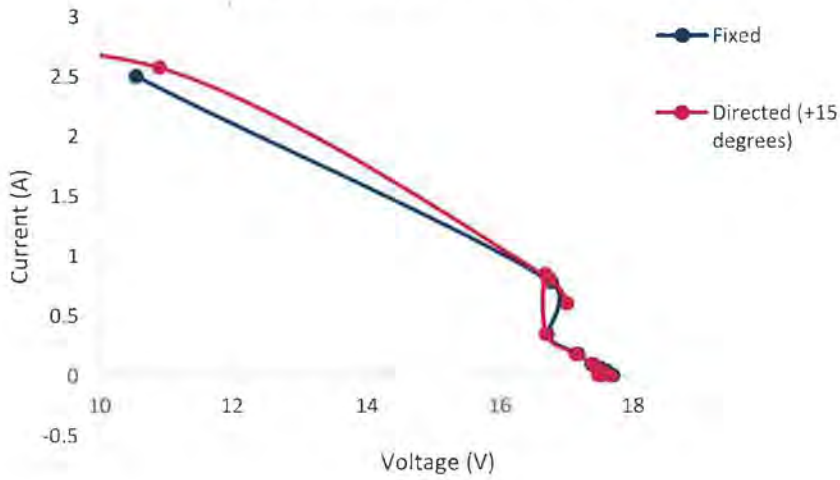




Data Set #2 | vs V: 10 am



Data Set #2 | vs V: 1 PM



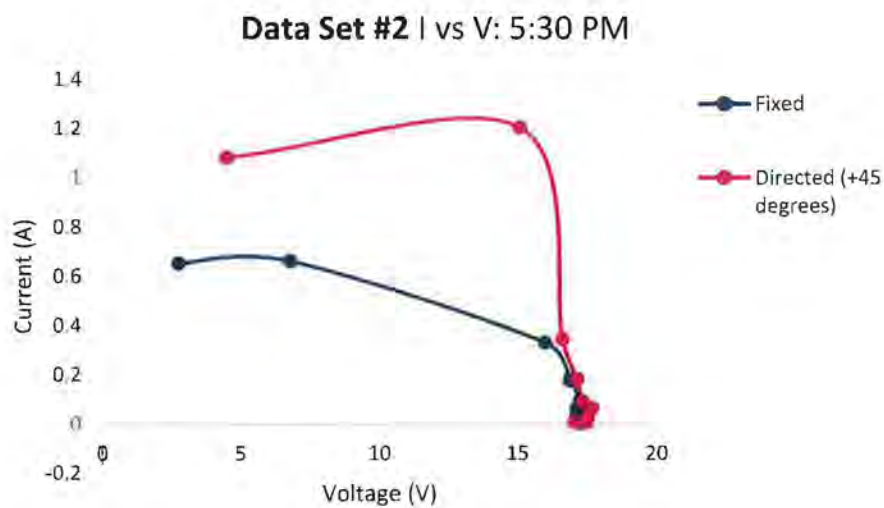
**Image Credits:**

Figure 1: ⁴

Figure 2: ²⁷

Figure 3: ¹⁴

Figure 4: ¹⁵

Figure 5-8: The author

Figure 9: ²⁸

Figure 10: ¹

Figure 11-13: The author via Autodesk Inventor [®]

Bibliography:

- (1) Cheng, T.-C.; Hung, W.-C.; Fang, T.-H. Two-Axis Solar Heat Collection Tracker System for Solar Thermal Applications <https://www.hindawi.com/journals/ijp/2013/803457/> (accessed Apr 23, 2019). <https://doi.org/10.1155/2013/803457>.
- (2) How do Photovoltaics Work? | Science Mission Directorate <https://science.nasa.gov/science-news/science-at-nasa/2002/solarcells> (accessed Apr 10, 2019).
- (3) *Spacecraft and Solar Cell Arrays*; NASA Space Vehicle Design Criteria (Guidance and Control) NASA SP-8074; NASA-Langley, 1971.
- (4) NASA History Division. Success and After: Chapter 12 <https://history.nasa.gov/SP-4202/chap12.html> (accessed Apr 7, 2019).
- (5) Mousazadeh, H.; Keyhani, A.; Javadi, A.; Mobli, H.; Abrinia, K.; Sharifi, A. A Review of Principle and Sun-Tracking Methods for Maximizing Solar Systems Output. *Renewable and Sustainable Energy Reviews* **2009**, *13* (8), 1800–1818. <https://doi.org/10.1016/j.rser.2009.01.022>.
- (6) How Solar Cells Work <https://science.howstuffworks.com/environmental/energy/solar-cell.htm> (accessed Apr 10, 2019).
- (7) How do solar cells work? | Explore | physics.org <http://www.physics.org/article-questions.asp?id=51> (accessed Apr 1, 2019).
- (8) How PV Cells Are Made http://www.fsec.ucf.edu/en/consumer/solar_electricity/basics/how_cells_made.htm (accessed Mar 30, 2019).
- (9) Jhee Phong Lee; Nasrudin Abd Rahim; Yusuf Al-Turki. (PDF) Performance of Dual-Axis Solar Tracker versus Static Solar System by Segmented Clearness Index in Malaysia | Academic Article https://www.researchgate.net/publication/270675496_Performance_of_Dual-Axis_Solar_Tracker_versus_Static_Solar_System_by_Segmented_Clearness_Index_in_Malaysia (accessed Mar 21, 2019). <http://dx.doi.org/10.1155/2013/820714>.
- (10) Homer Energy. Published Solar Data https://www.homerenergy.com/products/pro/docs/3.9/published_solar_data.html (accessed Mar 21, 2019).
- (11) Monocrystalline vs. Polycrystalline Solar Panels - What's the Difference? <https://www.altestore.com/video/monocrystalline-vs-polycrystalline-solar-panels-whats-the-difference-v63/> (accessed Mar 30, 2019).
- (12) Which Solar Panel Type Is Best? Mono-, Polycrystalline or Thin Film? *Energy Informative*.
- (13) How solar cell is made - material, manufacture, making, used, parts, structure, procedure, steps <http://www.madehow.com/Volume-1/Solar-Cell.html> (accessed Mar 30, 2019).
- (14) José R. Santiago Anadón. Large Force Shape Memory Alloy Linear Actuator, University of Florida, 2002.
- (15) Petrini, L.; Migliavacca, F. Biomedical Applications of Shape Memory Alloys <https://www.hindawi.com/journals/jm/2011/501483/> (accessed Mar 23, 2019). <https://doi.org/10.1155/2011/501483>.
- (16) Robotshop. Flexinol Technical Data Sheet <https://www.robotshop.com/media/files/pdf/flexinol-technical-data.pdf>.
- (17) NiTi Tension Springs, 4-pack http://store-musclewires-com.3dcartstores.com/NiTi-Tension-Springs-4-pack-_p_243.html (accessed Apr 22, 2019).
- (18) AltE. *What Can I Power with a 100W Solar Panel?*
- (19) Solar Insolation Map: How Many Sun Hours Do You Get? <https://www.wholesalesolar.com/solar-information/sun-hours-us-map> (accessed Mar 21, 2019).

- (20) AltE. Solar Charge Controllers - MPPT & PWM Controllers | altE /store/charge-controllers/solar-charge-controllers-c892/ (accessed Mar 21, 2019).
- (21) Charles Landau. Optimum Tilt of Solar Panels <http://solarpaneltilt.com/> (accessed Mar 21, 2019).
- (22) Greenstream Publishing. Solar Angle Calculator <http://solarelectricityhandbook.com/solar-angle-calculator.html> (accessed Mar 21, 2019).
- (23) The Modules of a Gear. February 13, 2010.
- (24) Commercial & Precision Worms (metric) | A 1C 5MYK10RB http://shop.sdp-si.com/catalog/product/?id=A_1C_5MYK10RB (accessed Apr 23, 2019).
- (25) Bevel and Miter Gears Selection Guide | Engineering360 https://www.globalspec.com/learnmore/motion_controls/power_transmission/gears/bevel_miter_gears (accessed Apr 23, 2019).
- (26) Corporation, I. Selecting Non-Metallic Gears From Nylon, Phenolic, Acetal, or PEEK <http://www.intechpower.com/products/gears/selecting-non-metallic-gears> (accessed Apr 23, 2019).
- (27) Visa, I.; Cotorcea, A.; Moldovan, M.; Neagoe, M. Two Degrees of Freedom Parallel Linkage to Track Solarthermal Platforms Installed on Ships. *IOP Conference Series: Materials Science and Engineering* **2016**, *147*, 012071. <https://doi.org/10.1088/1757-899X/147/1/012071>.
- (28) Samlex Solar. Power Curves & Characteristics for Solar Cells <https://www.samlexsolar.com/learning-center/solar-panels-characteristics.aspx> (accessed Apr 23, 2019).